Failure of Local Thermal Equilibrium in Quantum Friction

F. Intravaia,[1] R. O. Behunin,[2] C. Henkel,[3] K. Busch,[1,4] and D. A. R. Dalvit[5]
[1]*Max-Born-Institut, 12489 Berlin, Germany*
[2]*Department of Applied Physics, Yale University, New Haven, Connecticut 06511, USA*
[3]*Institute of Physics and Astronomy, University of Potsdam, Karl-Liebknecht-Str. 24/25, 14476 Potsdam, Germany*
[4]*Humboldt-Universität zu Berlin, Institut für Physik, AG Theoretische Optik & Photonik, 12489 Berlin, Germany*
[5]*Theoretical Division, MS B213, Los Alamos National Laboratory, Los Alamos, New Mexico 87545, USA*

(Received 10 May 2016; published 1 September 2016)

Recent progress in manipulating atomic and condensed matter systems has instigated a surge of interest in nonequilibrium physics, including many-body dynamics of trapped ultracold atoms and ions, near-field radiative heat transfer, and quantum friction. Under most circumstances the complexity of such nonequilibrium systems requires a number of approximations to make theoretical descriptions tractable. In particular, it is often assumed that spatially separated components of a system thermalize with their immediate surroundings, although the global state of the system is out of equilibrium. This powerful assumption reduces the complexity of nonequilibrium systems to the local application of well-founded equilibrium concepts. While this technique appears to be consistent for the description of some phenomena, we show that it fails for quantum friction by underestimating by approximately 80% the magnitude of the drag force. Our results show that the correlations among the components of driven, but steady-state, quantum systems invalidate the assumption of local thermal equilibrium, calling for a critical reexamination of this approach for describing the physics of nonequilibrium systems.

DOI: 10.1103/PhysRevLett.117.100402

In recent years the physics of nonequilibrium systems has attracted a lot of attention from different disciplines, such as stochastic thermodynamics and many-body quantum dynamics [1–3]. In particular, there has been a renewed interest in nonequilibrium dispersion forces. Better known for equilibrium phenomena such as the van der Waals and Casimir-Polder force [4] as well as the Casimir effect [5], these interactions play an important role in several fields of physics, including atomic [6] and statistical physics [7,8], gravitation [9], and cosmology [10]. Nonequilibrium physics enters in the description of these phenomena when, for example, temperature gradients or mechanical motion become relevant elements of the system.

From the theoretical standpoint, one must often rely on approximations in order to predict the nonequilibrium physics of a specific system. One of the most ubiquitous approaches relies on the local thermal equilibrium (LTE) approximation, which consists in treating the individual components of a system as if they were in local thermal equilibrium with their immediate surroundings. The main advantage of such a technique is that common equilibrium tools, such as the fluctuation-dissipation theorem (FDT) [11], can be applied locally, and then these local results are combined to describe the nonequilibrium dynamics of the full system. The usual justification for the LTE approximation is that the correlation length of the fields that mediate the interactions is often rather short (the dynamics in sufficiently well-separated locations are incoherent and can be treated as being independent [12,13]), and the subsystems locally relax to equilibrium on a fast time scale. The LTE approximation has been used in several nonequilibrium contexts, such as near-field radiative heat transfer [12], Casimir forces between bodies at different temperatures [14,15], and quantum friction [16–21]. In all these cases, however, a quantitative assessment of the LTE approximation is missing. In the present work, we show that this common approach actually fails to provide reliable predictions for quantum friction.

Let us consider an atom moving in vacuum with nonrelativistic velocity $\mathbf{v}$ at a distance $z_a > 0$ above and parallel to a flat surface placed at $z = 0$ (see Fig. 1). The atom couples to the electromagnetic field via its dipole moment $\hat{\mathbf{d}}(t)$ (the hat indicates a quantum operator). The frictional force can be obtained from the expectation value of the Lorentz force on the moving atom [22,23]. In our case this is equivalent to $\mathbf{F}_{\text{fric}} = \lim_{t\to\infty} \sum_i \langle \hat{d}_i(t) \nabla_\parallel \hat{E}_i(\mathbf{r}_a(t), t)\rangle$, where $\mathbf{r}_a(t)$ is the instantaneous position of the atom. In previous work [24] it was shown that this force at zero temperature (quantum friction) can be written as

$$\mathbf{F}_{\text{fric}} = -2 \int_0^\infty d\omega \int \frac{d^2\mathbf{k}}{(2\pi)^2} \times \mathbf{k}\,\mathrm{Tr}[\underline{S}(\mathbf{k}\cdot\mathbf{v} - \omega; \mathbf{v}) \cdot \underline{G}_I(\mathbf{k}, z_a, \omega)]. \tag{1}$$

Here, $\underline{S}(\omega; \mathbf{v})$ is the nonequilibrium velocity-dependent dipole power spectrum tensor (related to the spectral distribution of energy in the dipole), and $\underline{G}(\mathbf{k}, z_a, \omega)$ is the Fourier transform [in time and along the (x, y) plane] of

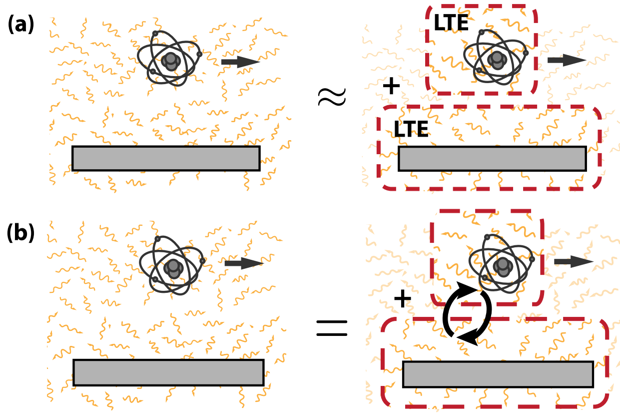

FIG. 1. Schematic representation of the difference between the LTE approximation (a) and the full nonequilibrium description (b) for quantum friction. In the first case it is assumed that the atom and the surface are separately in thermal equilibrium with their immediate local environments. This description applies the fluctuation-dissipation theorem for each subsystem, to approximately describe the full nonequilibrium system. Correlations between the atom and surface [pictorially represented by the black arrows in (b)] lead to a failure of the LTE approximation, which underestimates the magnitude of quantum friction by approximately 80% (see the main text).

the Green tensor describing the electromagnetic response of the surface. In the following the subscript I (R) means that the imaginary (real) part has to be (component-wise) considered, while "Tr" traces over tensor indices.

The standard approach used in the literature to compute the frictional force has been to resort to the LTE approximation. It is assumed that the particle and the surface surrounded by its electromagnetic field are *locally* in thermal equilibrium at $T = 0$ in their respective rest frames, and that the fluctuation-dissipation theorem separately applies to each subsystem [18–21]. In this case one assumes that $\underline{S}(\omega;\mathbf{v})$ is related to the imaginary part of the particle's polarizability tensor $\underline{\alpha}(\omega;\mathbf{v})$ via the zero-temperature FDT,

$$\underline{S}(\omega;\mathbf{v}) \approx \frac{\hbar}{\pi}\theta(\omega)\underline{\alpha}_I(\omega;\mathbf{v}) \tag{2}$$

[the function $\theta(\omega)$ is the Heaviside function]. In this LTE approximation, the frictional force at low velocities takes the form [24]

$$F_{\mathrm{fric}} \approx -\frac{2\hbar v^3}{3(2\pi)^3}\int_{-\infty}^{\infty} dk_y \int_0^{\infty} dk_x k_x^4 \mathrm{Tr}[\underline{\alpha}'_I(0)\cdot\underline{G}'_I(\mathbf{k},z_a,0)], \tag{3}$$

where the primes denote frequency derivatives and we assumed that the motion is along the x direction. A detailed evaluation of Eq. (3) requires the low-frequency behavior of the polarizability, which is often calculated within second-order perturbation theory [22,25–27]. Although the use of the LTE approximation can be justified within a second-order perturbative approach in the dipole strength for particles with large intrinsic dissipation [28], it becomes less rigorous for atoms, where dissipation is induced by the interaction with the electromagnetic field. For systems where radiative damping dominates, quantum friction requires a higher-than-second-order perturbative calculation: Since this necessarily encompasses correlations between the atom and the surface (see Fig. 1), one can expect in this case a failure of the local thermal equilibrium approximation. This is the key insight of this Letter.

In order to test the validity of the LTE approximation in quantum friction, we compute the dipole power spectrum $\underline{S}(\omega;\mathbf{v})$, evaluate the resulting drag force, and compare it to the LTE result. This entails the computation of the nonequilibrium steady state (NESS) of the joint atom + field + matter system. This difficult problem becomes manageable by modeling the internal atomic dynamics as a harmonic oscillator [29,30], for which it is possible to obtain an exact, nonperturbative form for the dipole power spectrum thanks to the quadratic nature of the full system Hamiltonian [24]. We work in the Heisenberg picture to calculate the dipole correlator in the steady state and then derive the power spectrum.

For simplicity, we consider a dipole with a fixed direction moving along a prescribed trajectory $\mathbf{r}_a(t) = (\mathbf{r}_a^{\parallel}(t), z_a)$. In the nonrelativistic approximation the dipole operator's equation of motion is given by

$$\partial_t^2\hat{\mathbf{d}}(t) + \omega_a^2\hat{\mathbf{d}}(t) = \omega_a^2\underline{\alpha}_0\cdot\hat{\mathbf{E}}(\mathbf{r}_a(t),t), \tag{4}$$

where ω_a is the oscillator's frequency, $\hat{\mathbf{E}}$ is the electric field, and $\underline{\alpha}_0$ is the static polarizability tensor, assumed to be symmetric for simplicity (it is proportional to a projector parallel to the direction of the dipole moment). We assume that the oscillator has no intrinsic dissipation—all dissipative dynamics arise from the coupling to the electromagnetic field. The electric field at the position of the atom is given by

$$\hat{\mathbf{E}}(\mathbf{r}_a(t),t) = \hat{\mathbf{E}}_0(\mathbf{r}_a(t),t) + \int_{t_i}^{t} dt' \int_{-\infty}^{\infty} d\omega e^{-i\omega(t-t')} \times \int \frac{d^2\mathbf{k}}{(2\pi)^2}\underline{G}(\mathbf{k},z_a,\omega)\cdot\hat{\mathbf{d}}(t')e^{i\mathbf{k}\cdot(\mathbf{r}_a^{\parallel}(t)-\mathbf{r}_a^{\parallel}(t'))}, \tag{5}$$

where $\hat{\mathbf{E}}_0$ is the field that is generated by the quantum fluctuating currents in the medium, while the second term is the field induced by the dipole and scattered by the surface. In the stationary $t \to \infty$ limit, we use that $\mathbf{r}_a^{\parallel}(t) \approx \mathbf{r}_a^{\parallel} + \mathbf{v}t$. Upon inserting (5) into the equation of motion for the dipole, we obtain the stationary solution in Fourier space as

$$\hat{\mathbf{d}}(\omega) = \int \frac{d^2\mathbf{k}}{(2\pi)^2}\underline{\alpha}(\omega;\mathbf{v})\cdot\hat{\mathbf{E}}_0(\mathbf{k},z_a,\omega+\mathbf{k}\cdot\mathbf{v})e^{i\mathbf{k}\cdot\mathbf{r}_a^{\parallel}}, \tag{6}$$

where we have defined the velocity-dependent polarizability

$$\underline{\alpha}(\omega;\mathbf{v}) = \frac{\omega_a^2}{\omega_a^2 - \Delta(\omega;\mathbf{v}) - \omega^2 - i\omega\gamma(\omega;\mathbf{v})}\underline{\alpha}_0. \quad (7)$$

In this expression, γ is the radiative damping while Δ is related to a frequency shift [24,31], and they are given by

$$\Delta(\omega;\mathbf{v}) = \omega_a^2 \int \frac{d^2\mathbf{k}}{(2\pi)^2}\mathrm{Tr}[\underline{\alpha}_0 \cdot \underline{G}_R(\mathbf{k}, z_a, \omega + \mathbf{k}\cdot\mathbf{v})], \quad (8a)$$

$$\gamma(\omega;\mathbf{v}) = \frac{\omega_a^2}{\omega} \int \frac{d^2\mathbf{k}}{(2\pi)^2}\mathrm{Tr}[\underline{\alpha}_0 \cdot \underline{G}_I(\mathbf{k}, z_a, \omega + \mathbf{k}\cdot\mathbf{v})]. \quad (8b)$$

The dipole correlation tensor, derived from Eq. (6), defines the power spectrum $\langle \hat{\mathbf{d}}(\omega)\hat{\mathbf{d}}(\omega')\rangle \equiv (2\pi)^2 \underline{S}(\omega;\mathbf{v})\delta(\omega+\omega')$, where the average is taken over the initial factorized state of the system, $\hat{\rho}(t_i) = \hat{\rho}_a(t_i) \otimes \hat{\rho}_{\mathrm{f/m}}(t_i)$. Here, $\hat{\rho}_a(t_i)$ is the atom's initial density matrix and $\hat{\rho}_{\mathrm{f/m}}(t_i)$ represents the state of the coupled field plus matter subsystem. Both the atom and the field + matter are assumed to be initially in their respective ground states. Using Eq. (6), we can compute the dipole-dipole correlation in terms of the $\hat{\mathbf{E}}_0$ field correlator, and since this field is solely generated by the static surface its correlator can be evaluated using the usual equilibrium FDT. In this way we derive the following expression for the power spectrum of the moving atom (see Supplemental Material [32]):

$$\underline{S}(\omega;\mathbf{v}) = \frac{\hbar}{\pi}\theta(\omega)\underline{\alpha}_I(\omega;\mathbf{v}) + \frac{\hbar}{\pi}\underline{J}(\omega;\mathbf{v}), \quad (9)$$

where

$$\underline{J}(\omega;\mathbf{v}) = \int \frac{d^2\mathbf{k}}{(2\pi)^2}[\theta(\omega + \mathbf{k}\cdot\mathbf{v}) - \theta(\omega)] \times \underline{\alpha}(\omega;\mathbf{v}) \cdot \underline{G}_I(\mathbf{k}, z_a, \omega + \mathbf{k}\cdot\mathbf{v}) \cdot \underline{\alpha}^*(\omega;\mathbf{v}). \quad (10)$$

Equation (9) constitutes the *generalized nonequilibrium* FDT for the moving harmonic oscillator. It shows that, when the system is in a NESS, an extra term $\underline{J}$ is added to the standard FDT, Eq. (2). The expression in (9) is similar to classical nonequilibrium generalizations of the FDT (see, for example, Refs. [33–37]), where the additional term is related to entropy production. However, these works often include assumptions (e.g., Markovianity) which are incompatible with the description of quantum friction [28].

Upon inserting Eq. (9) into (1), we obtain two distinct contributions to the quantum frictional force,

$$\mathbf{F}_{\mathrm{fric}} = \mathbf{F}_{\mathrm{fric}}^{\mathrm{LTE}} + \mathbf{F}_{\mathrm{fric}}^{J}, \quad (11)$$

which respectively arise from the first and second terms on the right-hand side of (9). As we will show below, the low-velocity expansion of $\mathbf{F}_{\mathrm{fric}}^{\mathrm{LTE}}$ corresponds to Eq. (3) [17,21,38], while $\mathbf{F}_{\mathrm{fric}}^{J}$ is entirely due to the nonequilibrium dynamics of our system. We assume that the motion occurs along the x direction, so that $\mathbf{F}_{\mathrm{fric}} = F_{\mathrm{fric}}\mathbf{x}$, (here $\mathbf{x}$, and below $\mathbf{y}$ and $\mathbf{z}$, are the unit vectors along the corresponding directions). The total Green tensor in Eq. (1) can be decomposed as the sum of the vacuum $\underline{G}_0$ and the scattered contribution $\underline{g}$ [39]. Because of Lorentz invariance, $\underline{G}_0$ does not contribute to the frictional force [38,40–42]. For simplicity, we consider the near-field limit for $\underline{g}$, which has an imaginary part that for our calculation can be written as [32]

$$\underline{g}_I(\mathbf{k}, z_a;\omega) = \frac{r_I(\omega)}{2\epsilon_0} k e^{-2kz_a}\left(\frac{k_x^2}{k^2}\mathbf{xx} + \frac{k_y^2}{k^2}\mathbf{yy} + \mathbf{zz}\right), \quad (12)$$

where $k = |\mathbf{k}| = \sqrt{k_x^2 + k_y^2}$, ϵ_0 is the vacuum permittivity, and $r(\omega)$ is the quasistatic approximation of the transverse magnetic reflection coefficient for the planar surface. Using the previous expression one can show that in the low-velocity limit the first term on the right-hand side of (11) gives (see Supplemental Material [32])

$$\bar{F}_{\mathrm{fric}}^{\mathrm{LTE}} \approx -\frac{90\bar{\mathcal{A}}^{\mathrm{LTE}}}{\pi^3}\hbar\alpha_0^2\rho^2\frac{v^3}{(2z_a)^{10}}, \quad (13)$$

where $\alpha_0 = \mathrm{Tr}[\underline{\alpha}_0]/3$ is the static isotropic (i.e., averaged over the solid angle) atomic polarizability, ρ is the material resistivity, and $\bar{\mathcal{A}}^{\mathrm{LTE}} = 21/20 \approx 1$ is the average over the solid angle of a geometrical factor describing the dipole's orientation [32]. Equation (3) reduces to the above expression when we use the polarizability given in (7). For the nonequilibrium correction term in Eq. (11), we obtain similarly [32]

$$\bar{F}_{\mathrm{fric}}^{J} \approx -\frac{72\bar{\mathcal{A}}^{J}}{\pi^3}\hbar\alpha_0^2\rho^2\frac{v^3}{(2z_a)^{10}}, \quad (14)$$

where $\bar{\mathcal{A}}^{J} = 87/80$. Adding the low-velocity expansions of $\bar{F}_{\mathrm{fric}}^{\mathrm{LTE}}$ and $\bar{F}_{\mathrm{fric}}^{J}$, the full quantum frictional force becomes

$$\bar{F}_{\mathrm{fric}} \approx -\frac{864}{5\pi^3}\hbar\alpha_0^2\rho^2\frac{v^3}{(2z_a)^{10}}, \quad (15)$$

which differs by almost a factor of two from the approximate LTE result in Eq. (13). This is the main result of our paper and demonstrates that the nonequilibrium contribution to the frictional force is certainly *not* negligible.

In Fig. 2 we depict the quantum frictional force Eq. (1) as a function of velocity. For simplicity the dipole is oriented along a specific direction (see caption of Fig. 2 and Supplemental Material [32]) and moving above a metallic surface described by the Drude model permittivity $\epsilon(\omega) = 1 - \omega_p^2[\omega(\omega + i\Gamma)]^{-1}$, where ω_p is the plasma frequency

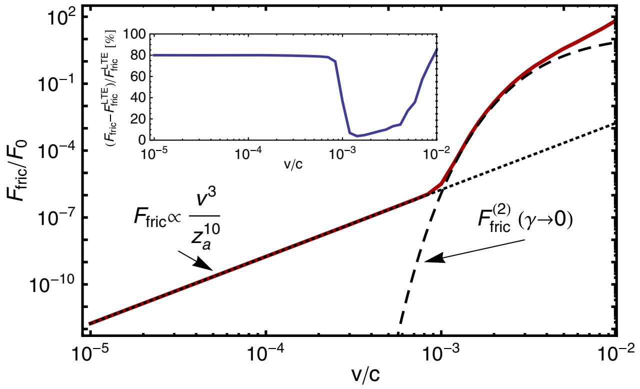

FIG. 2. Velocity dependence of the (normalized) quantum friction of a harmonic oscillator that moves with velocity v above a metallic surface described by the Drude model. The dipole is oriented along one of the directions for which $d_x^2 = d_y^2 = d_z^2$, e.g., $(1/\sqrt{3},\ 1/\sqrt{3},\ 1/\sqrt{3})$. The oscillator has a resonance frequency $\omega_a/\omega_{\rm sp} = 0.2$ and moves at a distance $z_a\omega_{\rm sp}/c = 0.05$ above and parallel to the surface with dissipation rate $\Gamma/\omega_{\rm sp} = 0.1$. At low velocities the LTE approximation underestimates the frictional force by approximately 80% (see inset). As the velocity increases ($v/c \gtrsim 10^{-3}$ for the parameters above), the oscillator's radiative damping becomes less relevant and the force is accurately described by the asymptotic expression given in Eq. (16) (dashed black line), which corresponds to $\gamma \to 0$. A further increase in the velocity enhances the nonequilibrium contribution to the force and a deviation from the LTE description occurs again (see inset). The normalization is $F_0 = -3\hbar\omega_{\rm sp}^5\alpha_0/(2\pi\epsilon_0 c^4)$. For a ^{87}Rb atom ($\alpha_0 = 5.26 \times 10^{-39}$ F m^2 [43]) and a plasma frequency $\omega_p = 9$ eV, we have $F_0 = 0.31$ fN.

and Γ is the metal's relaxation rate [in this case the material resistivity is given by $\rho = \Gamma/(\epsilon_0\omega_p^2)$]. For small velocities the friction is well described by the asymptotic expression Eq. (15) (black dotted line). In this region the integrals in Eq. (1) are dominated by the low frequency behavior of $\underline{S}(\omega;\mathbf{v})$ and $\underline{G}(\mathbf{k}, z_a, \omega)$, resulting in the power-law dependency on velocity and separation [32]. The relative difference between the full nonequilibrium and LTE results is more than 80% in this region (see inset of Fig. 2). At high velocities ($v/c \gtrsim 10^{-3}$ for the parameters in Fig. 2) we observe a crossing between the previous asymptotic expressions and

$$F^{(2)}_{\rm fric} \approx -\frac{\hbar\omega_{\rm sp}^4\alpha_0}{\pi c^4}\frac{\Gamma}{16\epsilon_0} \times \sqrt{\frac{\left(\frac{\omega_a}{\omega_{\rm sp}}\right)^7}{\pi\left(\frac{\omega_{\rm sp}z_a}{c}\right)^5\left(\frac{v}{c}\right)^3}}\left(1 + \frac{5v}{2z_a\omega_a}\right)e^{-(2z_a\omega_a/v)} \tag{16}$$

(black dashed curve in Fig. 2), where $\omega_{\rm sp} = \omega_p/\sqrt{2}$ is the surface plasmon frequency. Equation (16) is the result of a second-order perturbative expansion of Eq. (1), and can be explained by a resonant process involving the atom-surface interaction [28], for which the radiative damping is neglected. This process is dominant right after the crossing, as exemplified by the very good agreement between Eq. (16) and the numerical evaluation of quantum friction in this range of velocities. This agreement indicates that the atom and the surface are uncorrelated to a good approximation and hence that, in contrast to the lower-speed region, for these velocities the LTE description is sufficient to completely characterize the quantum frictional process. This is also clearly seen in the sharp decrease of the relative difference between the exact and LTE results (see inset of Fig. 2). In Fig. 2 one can see, however, that further increase of the velocity leads again to a deviation from the LTE approximation due to the strengthening of the nonequilibrium-induced atom-surface correlations.

Due to its small value, an experimental detection of quantum friction is challenging and designing setups that increase the strength of the interaction is certainly desirable. Specifically, Eq. (15) can be rewritten as

$$\bar{F}_{\rm fric} \approx -\frac{216}{5\pi}\hbar\gamma^2(z_a)\frac{v^3}{(2z_a\omega_a)^4}, \tag{17}$$

where $\gamma(z_a) = \alpha_0\omega_a^2\rho/(4\pi z_a^3)$ is the leading-order (i.e., low-frequency and small-velocity) expansion of the function $\gamma(\omega;\mathbf{v})$ defined in Eq. (8b). This demonstrates that, at low velocities, quantum friction is proportional to the square of the induced decay rate. This feature suggests possible pathways to increase the strength of the quantum frictional force. For instance, material properties or geometric configurations, such as hyperbolic nanostructures [44], which are known for producing large Purcell factors, are potentially favorable for enhancing the quantum frictional force.

In conclusion, we have shown that the local thermal equilibrium approximation fails in quantum friction. We demonstrated this point with an exact solution to a model of a harmonic oscillator moving parallel to a surface, in which the LTE approach underestimates the quantum friction force by approximately 80%. Motion-induced atom-surface correlations are ultimately responsible for the breakdown of the local equilibrium assumption. It is worth emphasizing that, despite its extensive and often reasonable application, the LTE approximation relies more on phenomenological considerations than on quantitative estimations. Our results in quantum friction call for a critical assessment of the range of applicability of local thermal equilibrium in other nonequilibrium dispersion interactions. Such an analysis could potentially provide new insights and unravel important features of these and other nonequilibrium systems.

We acknowledge support by the LANL LDRD program, and by the Deutsche Forschungsgemeinschaft (DFG) through project B10 within the Collaborative Research Center (CRC) 951 Hybrid Inorganic/Organic Systems for Opto-Electronics (HIOS). F. I. further acknowledges financial support from the European Union Marie Curie People program through the Career Integration Grant No. PCIG14-GA-2013-631571. C. H. and F. I. acknowledge support from the DFG through the DIP program (Grant No. SCHM 1049/7-1). R. B. further acknowledges financial support provided by NSF MRSEC DMR-1119826, the Packard Fellowship for Science and Engineering as well as Yale University startup funding.

[1] T. Speck and U. Seifert, Europhys. Lett. **74**, 391 (2006).
[2] U. Seifert, Eur. Phys. J. B **64**, 423 (2008).
[3] M. Rigol, V. Dunjko, and M. Olshanii, Nature (London) **452**, 854 (2008).
[4] H. B. G. Casimir and D. Polder, Phys. Rev. **73**, 360 (1948).
[5] H. B. G. Casimir, Proc. K. Ned. Akad. Wet. **51**, 793 (1948).
[6] J. Fortágh and C. Zimmermann, Rev. Mod. Phys. **79**, 235 (2007).
[7] M. E. Fisher and P.-G. de Gennes, CR Acad. Sci. Ser. B **287**, 207 (1978).
[8] A. Gambassi, J. Phys. Conf. Ser. **161**, 012037 (2009).
[9] R. Onofrio, New J. Phys. **8**, 237 (2006).
[10] R. J. Adler, B. Casey, and O. C. Jacob, Am. J. Phys. **63**, 620 (1995).
[11] H. B. Callen and T. A. Welton, Phys. Rev. **83**, 34 (1951).
[12] D. Polder and M. Van Hove, Phys. Rev. B **4**, 3303 (1971).
[13] W. Eckhardt, Phys. Rev. A **29**, 1991 (1984).
[14] I. A. Dorofeyev, J. Phys. A **31**, 4369 (1998).
[15] J. M. Obrecht, R. J. Wild, M. Antezza, L. P. Pitaevskii, S. Stringari, and E. A. Cornell, Phys. Rev. Lett. **98**, 063201 (2007).
[16] J. B. Pendry, J. Phys. Condens. Matter **9**, 10301 (1997).
[17] A. I. Volokitin and B. N. J. Persson, Rev. Mod. Phys. **79**, 1291 (2007).
[18] J. S. Høye and I. Brevik, Europhys. Lett. **91**, 60003 (2010).
[19] M. F. Maghrebi, R. L. Jaffe, and M. Kardar, Phys. Rev. Lett. **108**, 230403 (2012).
[20] M. F. Maghrebi, R. Golestanian, and M. Kardar, Phys. Rev. A **88**, 042509 (2013).
[21] J. S. Høye and I. Brevik, Eur. Phys. J. D **68**, 61 (2014).
[22] S. Y. Buhmann, L. Knöll, D.-G. Welsch, and H. T. Dung, Phys. Rev. A **70**, 052117 (2004).
[23] D. J. Griffiths, *Introduction to Electrodynamics*, 3rd ed. (Prentice Hall, Upper Saddle River, New Jersey, 1999).
[24] F. Intravaia, R. O. Behunin, and D. A. R. Dalvit, Phys. Rev. A **89**, 050101(R) (2014).
[25] P. W. Milonni and R. W. Boyd, Phys. Rev. A **69**, 023814 (2004).
[26] G. Lach, M. DeKieviet, and U. D. Jentschura, Phys. Rev. Lett. **108**, 043005 (2012).
[27] U. D. Jentschura, G. Lach, M. De Kieviet, and K. Pachucki, Phys. Rev. Lett. **114**, 043001 (2015).
[28] F. Intravaia, R. O. Behunin, C. Henkel, K. Busch, and D. A. R. Dalvit, arXiv:1603.05165.
[29] A. Einstein and L. Hopf, Ann. Phys. (Berlin) **338**, 1105 (1910).
[30] F. Intravaia, arXiv:1604.02990.
[31] J. Klatt, R. Bennett, and S. Y. Buhmann, arXiv:1601.02765.
[32] See Supplemental Material at http://link.aps.org/supplemental/10.1103/PhysRevLett.117.100402 for more details.
[33] G. S. Agarwal, Z. Phys. **252**, 25 (1972).
[34] R. Chetrite, G. Falkovich, and K. Gawedzki, J. Stat. Mech. (2008) P08005.
[35] M. Baiesi, C. Maes, and B. Wynants, Phys. Rev. Lett. **103**, 010602 (2009).
[36] P. Talkner, M. Campisi, and P. Hänggi, J. Stat. Mech. (2009), P02025.
[37] U. Seifert and T. Speck, Europhys. Lett. **89**, 10007 (2010).
[38] G. Dedkov and A. Kyasov, Phys. Solid State **45**, 1815 (2003).
[39] J. M. Wylie and J. E. Sipe, Phys. Rev. A **30**, 1185 (1984).
[40] A. A. Kyasov and G. V. Dedkov, Nucl. Instrum. Methods Phys. Res., Sect. B **195**, 247 (2002).
[41] A. I. Volokitin and B. N. J. Persson, Phys. Rev. B **78**, 155437 (2008).
[42] G. Pieplow and C. Henkel, New J. Phys. **15**, 023027 (2013).
[43] D. A. Steck, Technical report, Oregon Center for Optics and Department of Physics, University of Oregon, http://steck.us/alkalidata/.
[44] F. Intravaia and K. Busch, Phys. Rev. A **91**, 053836 (2015).